Increase of Plasma VEGF after Intravenous Administration of Bevacizumab Is Predicted by a Pharmacokinetic Model

Marianne O. Stefanini[1], Florence T. H. Wu[1], Feilim Mac Gabhann[2], and Aleksander S. Popel[1]

Abstract

Vascular endothelial growth factor (VEGF) is one of the most potent cytokines targeted in antiangiogenic therapies. Bevacizumab, a recombinant humanized monoclonal antibody to VEGF, is being used clinically in combination with chemotherapy for colorectal, non–small cell lung and breast cancers, and as a single agent for glioblastoma and is being tested for other types of cancer in numerous clinical trials. It has been reported that the intravenous injection of bevacizumab leads to an increase of plasma VEGF concentration in cancer patients. The mechanism responsible for this counterintuitive increase has not been elucidated, although several hypotheses have been proposed. We use a multiscale systems biology approach to address this problem. We have constructed a whole-body pharmacokinetic model comprising three compartments: blood, normal tissue, and tumor tissue. Molecular interactions among VEGF-A family members, their major receptors, the extracellular matrix, and an anti-VEGF ligand are considered for each compartment. Diffusible molecules extravasate, intravasate, are removed from the healthy tissue through the lymphatics, and are cleared from the blood. *Cancer Res; 70(23); 9886–94. ©2010 AACR.*

Major Findings

Our model reproduces the experimentally observed increase of plasma VEGF following intravenous administration of bevacizumab and predicts this increase to be a consequence of intercompartmental exchange of VEGF, the anti-VEGF agent and the VEGF/anti-VEGF complex. Our results suggest that a fraction of the anti-VEGF drug extravasates, allowing the agent to bind the interstitial VEGF. When the complex intravasates (via a combination of lymphatic drainage and microvascular transport of macromolecules) and dissociates in the blood, VEGF is released and the VEGF concentration increases in the plasma. These results provide a new hypothesis on the kinetics of VEGF and on the VEGF distribution in the body caused by antiangiogenic therapies, as well as their mechanisms of action and could help in designing antiangiogenic therapies.

Authors' Affiliations: [1]Department of Biomedical Engineering, and [2]Institute for Computational Medicine and Department of Biomedical Engineering, Johns Hopkins University, Baltimore, Maryland

Corresponding Author: Aleksander S. Popel, Department of Biomedical Engineering, Johns Hopkins University School of Medicine, 720 Rutland Avenue, 611 Traylor Research Building, Baltimore, MD 21205. Phone: 410-955-6419; E-mail: apopel@jhu.edu.

Introduction

VEGF is a key factor in tumor angiogenesis, and it has become a major target of antiangiogenic cancer therapy (1). A large body of evidence suggests that the free plasma VEGF concentration is elevated several fold in cancer patients compared to healthy subjects (2). Therapies targeting VEGF have shown promising results in cancer. Bevacizumab (Avastin, Genentech Inc.), a recombinant humanized monoclonal antibody to VEGF, has demonstrated efficacy in colorectal cancer, non–small cell lung cancer, breast cancer, renal cell carcinoma, and glioblastoma. The drug has been approved by the Food and Drug Administration (FDA) for these indications under certain conditions in combination with chemotherapeutic agents and is being tested for other types of cancer and other conditions in numerous clinical trials.

Despite the growing clinical applications of bevacizumab, the mechanism of action of this anti-VEGF agent and that of other anti-VEGF large molecules is not sufficiently understood (3). Specifically, two important questions remain: whether the drug acts by sequestering VEGF in the blood, tumor interstitium or both; and whether, as a result, the VEGF concentration in these compartments is reduced to "normal" levels. Answering these questions would significantly contribute to understanding the mechanism of action not only at the molecular level, but also at the levels of tissue, organ, and whole body and would help in the design of anti-VEGF agents. Gordon and colleagues reported that the intravenous injection of bevacizumab led to an increase in serum total VEGF in clinical trials whereas free VEGF concentration was reduced (4). Since then, other groups have reported counterintuitive increases in the plasma VEGF level following bevacizumab

American Association for Cancer Research

Quick Guide to Equations and Assumptions

Key Equations

The molecular detailed compartmental model is described by nonlinear ordinary differential equations on the basis of the principles of chemical kinetics and biological transport (summarized in Supplement 1). The following example equation describes the change over time of the concentration of vascular endothelial growth factor VEGF$_{121}$ isoform in the interstitial space of the normal tissue, denoted by the subscript N. The blood compartment is denoted by the subscript B.

$$\frac{d[V_{121}]_N}{dt} = q^N_{V121} - k_{on,V121,R1}[V_{121}]_N[R_1]_N + k_{off,V121R1}[V_{121}R_1]_N$$
$$- k_{on,V121,R2}[V_{121}]_N[R_2]_N + k_{off,V121R2}[V_{121}R_2]_N$$
$$- k_{on,V121,R1N1}[V_{121}]_N[R_1N_1]_N + k_{off,V121R1N1}[V_{121}R_1N_1]_N$$
$$- k_{on,V121,A}[V_{121}]_N[A]_N + k_{off,V121A}[V_{121}A]_N$$
$$- \left(\frac{k_L + k^{NB}_{pV}S_{NB}}{U_N}\right)\frac{[V_{121}]_N}{K_{AV,N}} + k^{BN}_{pV}\frac{S_{NB}}{U_N}\frac{U_B}{U_p}[V_{121}]_B$$

The right-hand side terms represent: secretion of VEGF$_{121}$ isoform (q_{V121}); binding to VEGF$_{121}$ to its receptors (VEGFR1 and VEGFR2) and to the complex VEGFR1/NRP1; binding of VEGF$_{121}$ to the anti-VEGF agent A; and the intercompartmental transport of VEGF$_{121}$ by lymphatics (k_L) and microvascular permeability to macromolecules (k_p). $S_{N,B}$ and $K_{AV,N}$ represent the total surface of microvessels at the normal tissue/blood interface and the available volume fraction for VEGF$_{121}$ in the total volume U_N, respectively. The total volumes are denoted by U. The subscript p in U_p denotes plasma as distinct from blood. Note that, with this nomenclature, the ratio U_p/U_B represents the available fluid volume fraction for VEGF$_{121}$ in the blood.

The injection of the anti-VEGF agent occurs after establishment of a physiologic steady state ($t < 0$). At $t = 0$, the anti-VEGF agent is administered intravenously at a rate q_A for a duration $\Delta t_{infusion}$ (typically in minutes). The subscript T represents the tumor. The equation governing the change of the anti-VEGF agent concentration in the blood over time reads:

$$\frac{d[A]_B}{dt} = q_A - c_A[A]_B - k^{BN}_{pV}\frac{S_{NB}}{U_p}[A]_B + \left(\frac{k_L + k^{NB}_{pV}S_{NB}}{U_B}\right)\frac{[A]_N}{K_{AV,N}}$$
$$- k^{BT}_{pV}\frac{S_{TB}}{U_p}[A]_B + k^{TB}_{pV}\frac{S_{TB}}{U_B}\frac{[A]_T}{K_{AV,T}}$$
$$- k_{on,V121,A}[V_{121}]_B[A]_B + k_{off,V121A}[V_{121}A]_B$$
$$- k_{on,V121,A}[V_{165}]_B[A]_B + k_{off,V165A}[V_{165}A]_B$$

where q_A = total dose/($n \times \Delta t_{infusion}$) during the duration of each treatment $\Delta t_{infusion}$ and $q_A = 0$ for all other times (n = number of injections). The first two terms on the right-hand side are the intravenous infusion of anti-VEGF at a rate q_A and the clearance of anti-VEGF from the blood at a rate c_A. The next terms represent: drug extravasation; removal of anti-VEGF agent by lymphatics; and drug intravasation (when the intercompartment transports are included). The last two terms describe the binding of the anti-VEGF agent to both VEGF isoforms.

As a final example, the change over time of the corresponding VEGF/anti-VEGF concentration in the normal tissue when the extravasation of the anti-VEGF agent is governed by

$$\frac{d[V_{121}A]_N}{dt} = k_{on,V121,A}[V_{121}]_N[A]_N - k_{off,V121A}[V_{121}A]_N$$
$$- \left(\frac{k_L + k^{NB}_{pV}S_{NB}}{U_N}\right)\frac{[V_{121}A]_N}{K_{AV,N}} + k^{BN}_{pV}\frac{S_{NB}}{U_N}\frac{U_B}{U_p}[V_{121}A]_B$$

and is dependent on: VEGF$_{121}$ binding to the anti-VEGF agent; and transport of the VEGF/anti-VEGF complex between the compartments.

Major Assumptions of the Model

Our model does not represent a particular stage or type of cancer to keep the model general in light of the fact that bevacizumab is administered in primary and metastatic diseases and in adjuvant or neoadjuvant settings. Therefore, our tumor compartment can either be a primary tumor or the aggregate of metastases in tissue.

Because the simulation results for a smaller tumor (half the diameter of the tumor considered in this study) were not significantly different (both qualitatively and quantitatively--data not shown), our model does not consider the possible change in tumor volume that may result from the injection of the anti-VEGF agent for the duration of our simulations.

The degradation of VEGF by proteases is not currently included in the model. Effects of platelets and leukocytes as potential sites for sequestering VEGF, anti-VEGF, and their products are not considered and should also be added in the future. We assume that only endothelial cells express VEGF receptors. Our model does not include the presence of receptors on the luminal surface of endothelial cells and the quantification of abluminal receptors has been estimated from previous studies.

The model does not include multimeric binding of the anti-VEGF or the ability of the anti-VEGF to bind to matrix-bound VEGF. We assume that the anti-VEGF has a half-life of 21 days. Its complexes formed by the binding of $VEGF_{121}$ or $VEGF_{165}$ are assumed to have the same half-lives because bound and free bevacizumab exhibit the same pharmacokinetic profile. The binding and unbinding rates of the anti-VEGF to VEGF are taken from the literature to be 9.2×10^4 $(mol/L)^{-1} \cdot s^{-1}$ and 2.0×10^{-4} s^{-1}, respectively leading to a dissociation constant K_d of 2.2 nM. The above assumptions can be relaxed, if warranted by experimental data, within the framework of the model that is generally suitable for simulating anti-VEGF therapeutics.

administration (5–7). In the ocular setting, Campa and colleagues reported that intravitreal bevacizumab injection increased the VEGF concentration in the aqueous humor (8). Several hypotheses have been formulated to explain this phenomenon. Hsei and colleagues have suggested that the clearance of complexed VEGF is lower than that of free VEGF in rats and hypothesized that this lower clearance could explain the accumulation of total VEGF in serum (9). Other groups have suggested alternate pathways activated by the injection of bevacizumab, such as: accumulation of hypoxia-inducible factor leading to an increase of VEGF in serum, or secondary macular edema for the eye (8, 10, 11). Loupakis and colleagues immunodepleted plasma to remove bevacizumab and bevacizumab–VEGF complexes and found that plasma-free VEGF was significantly reduced after bevacizumab administration (12); this methodology helps to circumvent the problem that the ELISA method used in a number of studies cannot distinguish between free and total (including bevacizumab-bound) VEGF. The results of the study corroborate an earlier proposal by Christofanilli and colleagues (13) that free VEGF can serve as a surrogate marker.

Systems biology approaches, specifically computational and mathematical modeling, are emerging as powerful tools in fundamental studies of cancer and design of therapeutics (14, 15). To better understand VEGF distribution in the body, we have built a three-compartment model composed of normal (healthy) tissue, blood, and tumor (16). In this study, we have extended our computational model by including an anti-VEGF agent delivered by the intravenous infusion (i.e., into the blood compartment). The model describes the effect of such administration on the VEGF distribution in the blood, normal, and diseased tissues. Our goal is to understand how the distribution of VEGF, anti-VEGF agent, and their products changes following the agent administration; in particular, we will investigate whether the plasma VEGF level increases or decreases following an intravenous injection of the anti-VEGF agent.

Even though the results are presented using the parameters for bevacizumab, the model can be applied to other anti-VEGF agents. One such agent is aflibercept or VEGF Trap (Regeneron Pharmaceuticals Inc.), a soluble humanized VEGF receptor protein designed to bind all VEGF-A isoforms and placental growth factor (PlGF). This fusion protein serves as a soluble decoy receptor and is currently in clinical trials.

Our model includes two VEGF-A isoforms ($VEGF_{121}$ and $VEGF_{165}$), as well as VEGF receptors (VEGFR1 and VEGFR2) and the coreceptor neuropilin-1 (NRP1). In this study, we assume that VEGFR1, VEGFR2, and NRP1 are present only on the abluminal surface of the endothelial cells. The transcapillary microvascular permeability for the diffusible molecules (VEGF, anti-VEGF, and the VEGF/anti-VEGF complex) is included, as well as lymphatic drainage from the interstitial space into the blood compartment. The model equations are presented in the Supplemental Information (Supplement 1).

Materials and Methods

Most of the parameters for the anti-VEGF agent were taken from published data on bevacizumab. We assume a half-life of 21 days (4) for the anti-VEGF whether unbound or bound to $VEGF_{121}$ or $VEGF_{165}$, as bound and free bevacizumab exhibit the same pharmacokinetic profile (9). Kinetic parameters (k_{on}, k_{off}) for the binding and unbinding of the anti-VEGF to the vascular endothelial growth factor were taken to be 9.2×10^4 $(mol/L)^{-1} \cdot s^{-1}$ and 2.0×10^{-4} s^{-1} respectively, leading to a dissociation constant K_d of 2.2 nM (17).

Experiments have shown that bevacizumab may have multimeric binding to VEGF (9, 18) and can bind to extracellular matrix-sequestered VEGF (19). For simplicity purposes, we limit our model to monomeric binding to VEGF and neglect binding to VEGF sequestered by the extracellular matrix; these can be included when quantification of binding sites and the kinetics become available. Bevacizumab has also been reported to alter the VEGF-dependent microvascular permeability to soluble molecules (20). As a first approximation, we assume that the geometry of each tissue and the capillary density remains constant in the course of our simulations, that is, we do not include tissue remodeling after the injection of the anti-VEGF agent. Although it may be important, the inclusion of tissue remodeling would take the model beyond the scope of this study but could be of interest for further studies. This model does not include VEGF receptors on the luminal side of endothelial cells that have not been experi-

mentally characterized, but we have recently shown how such expression would alter the VEGF distribution (21); we do not expect that any qualitative conclusions of the study would be affected by the presence of luminal receptors.

Note that the simulations are not aimed at representing a particular type or stage of cancer, recognizing that VEGF-neutralizing agents may be administered in cases of both metastatic and primary tumors. Thus, in the model, the tumor compartment can represent either an aggregate volume of metastases or a primary tumor. Due to the wide range of possibilities that could be represented for different types and stages of cancer, we adopt the parameters for this compartment from our previous study (16) and conduct a sensitivity study to ascertain that our qualitative conclusions are not dependent on the choice of parameters.

For each simulation, the system was first equilibrated at a baseline for a cancer patient with tumor before the injection of the VEGF-neutralizing agent. At time zero, intravenous infusion of the anti-VEGF agent begins and delivery to the blood compartment continues as a slow infusion for 90 minutes. We considered two treatment regimens: a single-dose treatment of 10 mg/kg or 10 consecutive daily doses of 1 mg/kg (metronomic therapy).

The parameters and their assigned numerical values are summarized in Supplement 3. The equations governing the 3-compartment VEGF transport system have been described in our previous papers (16, 21) and can be found in Supplement 1. We have also added equations to describe the interactions and intercompartmental transport of the anti-VEGF molecule (Equations S.30–S.38).

Results

Experiments demonstrate an inverse relationship between microvascular permeability and the size of a molecule (molecular weight or Stokes–Einstein radius; refs. 22–24). Therefore, in the absence of active transport, large proteins, such as anti-VEGF agents (150 kDa for bevacizumab and 110 kDa for aflibercept), should extravasate relatively slowly. In apparent agreement with this, the level of bevacizumab following an intravenous injection has been observed to be several times lower in normal tissues (25) and in tumors (19) than in the blood. However, little is known about what role, if any, the extravasation of an anti-VEGF agent may play in the therapeutic mechanism. To address this issue, we considered two computational scenarios: in the first, the anti-VEGF agent is constrained in the blood compartment (negligible extravasation); in the second, the extravasation of the anti-VEGF agent is included.

Plasma-free VEGF is predicted to decrease following intravenous injection of an anti-VEGF agent confined to the blood compartment (no extravasation)

Changes in plasma- and tissue-free VEGF are summarized in Fig. 1A for a single-injection (10 mg/kg) and Fig. 1C for metronomic therapy (1 mg/kg daily for 10 days), that is, repeated lower doses over a longer period of time (26). Total amount of drug injected is the same in both scenarios.

If the anti-VEGF agent is confined to the blood compartment, a single injection causes the concentration of free VEGF (i.e., not bound to anti-VEGF) in plasma to decrease precipitously by 98.4% (Fig. 1A, dashed line; minimum as the infusion ends), as the anti-VEGF agent binds to VEGF available in plasma. However, this is not predicted to significantly affect the free VEGF level in the healthy tissue [maximum 0.1% drop at 9 hours (solid line)] or the free VEGF level in the tumor compartment [maximum 0.2% drop at 30 hours (dotted line)]. The free anti-VEGF agent saturated the blood (Supplementary Figure S1A) and reached a maximum of ~1.7 μmol/L in plasma (~88 μg/mL plasma) at the end of the infusion, which corresponds to the total injected amount of the 150-kDa agent distributed in the volume of plasma for a 70-kg patient. The VEGF/anti-VEGF complex reached its maximum concentration in the blood (~2.1 nmol/L) after about 12 days (Supplementary Figure S2A). The total (free and bound to the anti-VEGF agent) VEGF concentration is typically what is measured by VEGF ELISA methods (see Supplement 2 for a compilation of experimental data on free/total VEGF changes following bevacizumab administration). Our results show a 100- to 1,000-fold difference between free VEGF concentration (Fig. 1) and the concentration of VEGF bound to the anti-VEGF (Supplementary Figure S2). Because of this difference in magnitude, the unbound VEGF concentration represents only a small percentage of the total VEGF concentration, and thus Supplementary Figure S2 also illustrates the total VEGF concentration profile.

For metronomic therapy (lower daily dose of 1 mg/kg over 10 days), the free VEGF in plasma declines 86.8% following the first infusion, but is predicted to reach a pseudo-steady state after multiple infusions (Fig. 1C, dashed line). The concentration of free VEGF returned to its baseline level within 3 weeks once the treatment was stopped. Metronomic therapy showed delayed and lowered maximum levels of anti-VEGF compared to the single-dose regimen (Supplementary Figure S1C versus Supplementary Figure S1A); although the half-life of the anti-VEGF agent is relatively long, it is being cleared from plasma continuously. The VEGF/anti-VEGF complex (and therefore the total VEGF concentration) reached its maximum about a week later than for the single dose (Supplementary Figure S2C versus Supplementary Figure S2A).

For an anti-VEGF agent that extravasates, plasma-free VEGF is predicted to first decrease and then increase above the baseline level

As for a nonextravasating anti-VEGF agent (Fig. 1A), plasma-free VEGF decreased (97.0% drop in the first 45 minutes) following administration of anti-VEGF that can extravasate (Fig. 1B, dashed line), as the agent binds to the available free VEGF. In this case, however, VEGF concentration then rebounded to 41.1 pmol/L (a 9.1-fold increase over baseline) after about 1 week. Unlike the no-extravasation case where the concentration returned to baseline after 3 weeks, the free VEGF concentration in plasma was predicted to remain significantly elevated after 3 weeks (40.5 pmol/L, 9-fold the baseline level). The free VEGF concentration in the normal (solid line) and tumor (dotted line) tissues both also
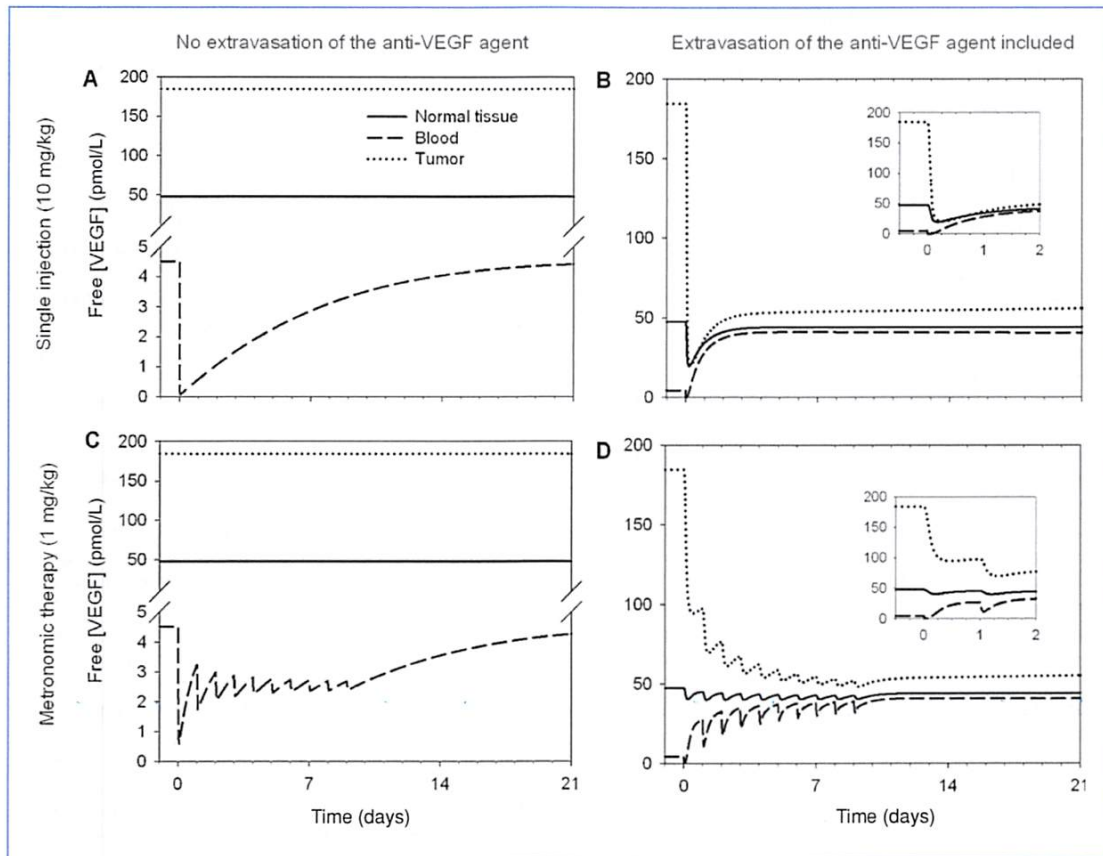
Figure 1. Free VEGF concentration profiles following the intravenous injection of an anti-VEGF agent. A and B, single injection (10 mg/kg). C and D, daily injection of 1 mg/kg for 10 days (metronomic therapy). One pmol/L of VEGF equivalent to 24 pg/mL of total blood. Solid line, normal tissue; dashed line, blood; dotted line: tumor.

showed an initial transient decrease (58.5% and 88.9%, respectively), followed by a slight rebound, reaching steady states 6.8% and 69.7% below baseline, respectively. This could be due to the long half-life of the anti-VEGF agent (21 days) as compared to the characteristic times of clearance, binding affinities, and internalization rates of VEGF receptors. This may suggest that an important whether not the primary action of the anti-VEGF agent is to deplete the tumor VEGF after the anti-VEGF extravasation. Interestingly, the increase of free VEGF in plasma is also predicted even in the absence of a tumor compartment (data not shown).

Supplementary Figure S1B shows the dynamic response of the free anti-VEGF agent concentration. Upon injection, the free anti-VEGF concentration at first increases but then decreases rapidly within the next 12 hours as it travels to the normal and tumor tissues. Interestingly, the free anti-VEGF concentrations in the blood and in the tumor were almost identical. This was mainly due to the higher microvascular permeability and the absence of functioning lymphatics in the tumor. The formation of the VEGF/anti-VEGF

complex (and the total VEGF concentration) reached a maximum after about 4 days and was significantly higher in the tumor than in the other compartments due to higher VEGF concentrations (Supplementary Figure S2B).

In metronomic therapy (Fig. 1D), similar results were observed. The free VEGF concentration decreased in the plasma upon the anti-VEGF injection then rebounded and increased further after each injection (dashed line). In the healthy and tumor compartments (solid and dotted lines, respectively), a decrease in the free VEGF concentration was observed, followed by a rebound effect without exceeding their respective baseline levels. In all three compartments, the free VEGF concentrations are predicted to reach a steady state at the end of the 10 days of treatment and then remain almost constant (varying within a small range) over the duration of the experiment: the free VEGF level in the tumor was significantly decreased ($\sim$70.1%), whereas that in the plasma was significantly increased (by 8-fold) as compared to the baseline. Although the rebound in free VEGF in plasma occurred after 45 minutes, the rebound still happens if we limit the duration

DOCKET ALARM

Explore Litigation Insights

Docket Alarm provides insights to develop a more informed litigation strategy and the peace of mind of knowing you're on top of things.

Real-Time Litigation Alerts

Keep your litigation team up-to-date with **real-time alerts** and advanced team management tools built for the enterprise, all while greatly reducing PACER spend.

Our comprehensive service means we can handle Federal, State, and Administrative courts across the country.

Advanced Docket Research

With over 230 million records, Docket Alarm's cloud-native docket research platform finds what other services can't. Coverage includes Federal, State, plus PTAB, TTAB, ITC and NLRB decisions, all in one place.

Identify arguments that have been successful in the past with full text, pinpoint searching. Link to case law cited within any court document via Fastcase.

Analytics At Your Fingertips

Learn what happened the last time a particular judge, opposing counsel or company faced cases similar to yours.

Advanced out-of-the-box PTAB and TTAB analytics are always at your fingertips.

API

Docket Alarm offers a powerful API (application programming interface) to developers that want to integrate case filings into their apps.

LAW FIRMS
Build custom dashboards for your attorneys and clients with live data direct from the court.

Automate many repetitive legal tasks like conflict checks, document management, and marketing.

FINANCIAL INSTITUTIONS
Litigation and bankruptcy checks for companies and debtors.

E-DISCOVERY AND LEGAL VENDORS
Sync your system to PACER to automate legal marketing.

fastcase
Smarter legal research.